



OPEN

Metabolomic insights in advanced cardiomyopathy of chronic chagasic and idiopathic patients that underwent heart transplant

Raphaella M. de Oliveira^{1,2}, Mariana U. B. Paiva¹, Carolina R. C. Picossi³, Diego V. N. Paiva¹, Carlos A. O. Ricart², Francisco J. Ruperez³, Coral Barbas³, Fernando A. Atik^{1,4} & Aline M. A. Martins^{1,3}✉

Heart failure (HF) studies typically focus on ischemic and idiopathic heart diseases. Chronic chagasic cardiomyopathy (CCC) is a progressive degenerative inflammatory condition highly prevalent in Latin America that leads to a disturbance of cardiac conduction system. Despite its clinical and epidemiological importance, CCC molecular pathogenesis is poorly understood. Here we characterize and discriminate the plasma metabolomic profile of 15 patients with advanced HF referred for heart transplantation – 8 patients with CCC and 7 with idiopathic dilated cardiomyopathy (IDC) – using gas chromatography/quadrupole time-of-flight mass spectrometry. Compared to the 12 heart donor individuals, also included to represent the control (CTRL) scenario, patients with advanced HF exhibited a metabolic imbalance with 21 discriminating metabolites, mostly indicative of accumulation of fatty acids, amino acids and important components of the tricarboxylic acid (TCA) cycle. CCC vs. IDC analyses revealed a metabolic disparity between conditions, with 12 CCC distinctive metabolites vs. 11 IDC representative metabolites. Disturbances were mainly related to amino acid metabolism profile. Although mitochondrial dysfunction and loss of metabolic flexibility may be a central mechanistic event in advanced HF, metabolic imbalance differs between CCC and IDC populations, possibly explaining the dissimilar clinical course of Chagas' patients.

Heart failure (HF) is a clinical syndrome associated with alterations in cardiac energy metabolism, such as imbalanced anabolic-catabolic signaling and defects in energy production¹, and significant phenotypic heterogeneity. One of the predisposing causes is non-ischemic dilated cardiomyopathy (DCM), which usually starts with a long preclinical phase that, regardless of etiology, progresses to hypertrophic remodeling and dilation and systolic dysfunction of the left or both ventricles². Attributed to genetic or non-genetic causes, as in idiopathic dilated cardiomyopathy (IDC) or myocarditis, the molecular spectrum common to DCM subtypes includes a stimulation of the sympathetic adrenergic and renin–angiotensin–aldosterone (RAAS) systems and mobilization of natriuretic peptides to increase vascular tone, inotropism and sodium and water retention³.

Among non-ischemic DCM etiologies, chronic chagasic cardiomyopathy (CCC) is highly prevalent in Latin America⁴. As a progressive degenerative inflammatory condition that primarily causes collagen accumulation in myocardial interstitium and disturbance of cardiac conduction system⁵, cardiac muscle involvement in CCC is complex. Heart remodeling occurs as a result of the synergistic effect between immunological and inflammatory factors, cardiac dysautonomia and microvascular disturbances⁵. A recent study also found that cardiomyocytes isolated from Chagas' patients have higher levels of intracellular inositol 1, 4, 5 trisphosphate (IP₃), a metabolite that stimulates a significantly increase in diastolic calcium ions (Ca²⁺) concentration and consequently aggravates the contractile disorder⁶.

In this context, metabolic fingerprints have great potential to improve the understanding and molecular signature of chagasic HF previously investigated by other omics^{7–9}. However, most reports focus on ischemic and idiopathic heart diseases, excluding patients with CCC despite their clinical and epidemiological importance.

¹School of Medicine, University of Brasilia, Brasilia, Brazil. ²Laboratory of Protein Chemistry and Biochemistry, University of Brasilia, Brasilia, Brazil. ³Center of Excellence in Metabolomics and Bioanalysis, University of San Pablo CEU, Madrid, Spain. ⁴Institute of Cardiology and Transplantation of the Federal District, Brasilia, Brazil. ✉email: alin3.m4rtins@gmail.com

Thus, the aim of our study was to characterize and discriminate possible molecular mechanistic events that drives the phenotypical result of non-ischemic HF and CCC patients using a metabolomics approach.

Results

Advanced HF vs. control (CTRL)

The baseline demographic and clinical characteristics of patients with advanced HF are shown in Table 1. With exception of age ($p = 0.03$), diastolic blood pressure ($p = 0.042$) and heart rate ($p = 0.02$), no significant differences were found between CCC and IDC patients. In multivariate statistics, the analytical reproducibility was confirmed by quality control (QC) samples clustering in principal component analysis (PCA) (Fig. 1A). Orthogonal partial least squares-discriminant analysis (OPLS-DA) revealed a differential metabolic profile in cardiac compromise, with $Q^2 = 0.83$ (Fig. 1B) and 21 HF discriminating metabolites (Fig. 1C). Differences in intensity and distribution of these compounds were demonstrated by heatmap (Fig. 1D) and box plot (Fig. 1E). Most of them belong to the class of fatty acids and conjugates or amino acids, peptides and analogues (Fig. 2A). Their interaction network indicated an interactome pathway potentially implicated in the pathophysiology of advanced non-ischemic HF (Fig. 2B). OPLS-DA results for each pathological scenario vs. CTRL subjects are shown in Supplemental Fig. 1 and the univariate findings in Supplemental Table 1.

CCC vs. IDC vs. CTRL

QC samples clustering attested the consistency of the experimental method in PCA (Fig. 3A). OPLS-DA identified distinct profiles for each condition, with greater distance between CCC and CTRL groups, with $Q^2 = 0.85$ (Fig. 3B). Variations in the relative intensity of 18 metabolites were crucial in characterizing the scenarios (Fig. 3C). The results of univariate analysis are shown in Supplemental Table 2.

CCC vs. IDC

The method's reliability was ratified by QC samples clustering in PCA (Fig. 4A). OPLS-DA revealed a metabolic discrimination between the pathological conditions, with $Q^2 = 0.54$ (Fig. 4B) and 12 CCC distinctive metabolites vs. 11 IDC representative metabolites (Fig. 4C). Differences in intensity and distribution of these compounds were confirmed by heatmap (Fig. 4D) and box plot (Fig. 4E). The majority of CCC relatively intense metabolites belong to the class of carbohydrates and carbohydrate conjugates, while those important for IDC characterization mostly belong to the class of amino acids, peptides and analogues (Fig. 2C). CCC's metabolites interaction network suggested a possible pathway particularly associated with the pathophysiology of Chagas Disease (ChD)-related HF (Fig. 2D).

Discussion

Metabolite impairment in advanced HF pathophysiology

Although the clinical evolution of patients with ChD-related HF is worse compared to non-Chagas' patients¹⁰, the molecular features that differentiate the pathogenesis and, consequently, the clinical outcome of CCC and IDC have not yet been elucidated. Here, OPLS-DA results demonstrated that patients with advanced HF, regardless of the cause, exhibit a global metabolic disturbance (Fig. 1B) with higher abundance of 21 identified metabolites (Fig. 1C–E).

Under physiological conditions, the adult heart is metabolically flexible and generates adenosine triphosphate (ATP) from several substrates, such as fatty acids (FAs), lactate, glucose, ketones and amino acids (AAs), obtained continuously from the blood and directed to mitochondrial oxidative phosphorylation (95%) and glycolysis (5%)^{11–13}. Up to 60% of mitochondrial ATP production results from FA oxidation, however due to its greater need for oxygen and compromised mitochondrial oxidative capacity, failing hearts tend to increase glucose consumption via anaerobic glycolysis as a compensatory mechanism for maintaining ATP levels^{11,13–16}. Metabolic reprogramming in HF also includes increased oxidation of ketone bodies and reduced oxidation of lactate, branched-chain amino acids (BCAA) and glucose, impairing overall ATP production by the tricarboxylic acid (TCA) cycle flux^{11,13}.

Indeed, the accumulation of FAs, AAs and important TCA cycle components (citric and succinic acids) observed in plasma of HF patients in the present study (Fig. 2A) suggests an important mitochondrial dysfunction and consequent loss of metabolic flexibility, which may contribute to the known reduction of up to 30% of ATP content in failing hearts^{11,13,17}. As channeled by HF's relatively intense metabolites network, these two major pathways may interact along as shown in Fig. 2B.

The effort to sustain energy demand during pathological hypertrophy leads to maladaptive circuits, such as increased mitochondrial protein acetylation, which produce mitochondrial stress and eventually mitochondria-initiated cell death¹⁸. From a clinical perspective, this metabolic remodeling may be expressed in left ventricle (LV) hypertrophy progression, as it decreases ventricular compliance and consequently increases filling pressure, in addition to constituting an arrhythmogenic substrate by disorganizing tissue cytoarchitecture¹⁹. Furthermore, free FAs concentration in plasma is independently associated with HF incidence and adverse outcome^{20,21}, and lipid moieties accumulation due to extrapolation of mitochondrial oxidative capacity may result in lipotoxicity and lead to myocardial dysfunction^{22,23}.

Metabolite impairment in CCC and IDC pathophysiology

Comparing CCC and IDC individually to CTRL samples, OPLS-DA results indicates a metabolic profile disparity between the pathological settings, with greater discrimination of CCC in relation to the physiological condition (Fig. 3B and C), corroborating the clinical observations on the outcome and prognosis of these patients^{24–26}. Other omics studies have also identified differences among HF etiologies. Cunha-Neto et al.²⁷ characterizing gene

Characteristics	CCC (n=8)	IDC (n=7)	p-value
Male sex	6 (75%)	4 (57.14%)	0.855
Age, y	56.6 (± 10.6)	29.3 (± 21.9)	0.03
Weight, kg	57.5 (± 12.5)	61.1 (± 20.9)	1
BMI, kg/m ²	21.2 (± 4.81)	22.7 (± 7.93)	1
NYHA functional class ^a	–	–	0.232
I/II	0(0%)	1 (14.29%)	–
III	4(50%)	2 (28.57%)	–
IV	4(50%)	4 (57.14%)	–
Hemodynamic profile ^b	–	–	0.935
A	1 (12.5%)	1 (14.29%)	–
B	4 (50%)	4 (57.14%)	–
C	3 (37.5%)	2 (28.57%)	–
History	–	–	–
Hypertension	1 (12.5%)	1 (14.29%)	1
Dyslipidemia	4 (50%)	1 (14.29%)	0.36
Myocardial infarction	0 (0%)	0 (0%)	–
Stroke	3 (37.5%)	1 (14.29%)	0.506
Current smoking	0 (0%)	1 (14.29%)	1
Atrial fibrillation	2 (25%)	2 (28.57%)	0.506
Physical examination	–	–	–
Systolic BP, mmHg	95.4 (± 16.8)	105 (± 12.8)	0.152
Diastolic BP, mmHg	58.4 (± 9.2)	71.9 (± 13)	0.042
Heart rate, beats/min	64.2 (± 11)	83.1 (± 18.6)	0.02
O ₂ saturation, %	99 (± 1)	99 (± 0.9)	0.7
Echocardiography	–	–	–
LVEF, %	26 (± 7)	25 (± 8)	0.955
LVDD, mm	69.4(± 7.76)	64 (± 9.19)	0.473
Diastolic dysfunction	6 (75%)	7 (100%)	0.344
Right ventricular dysfunction	8 (100%)	7 (100%)	–
Laboratory	–	–	–
Hemoglobin, g/dL	12.7 (± 2.29)	12.1 (± 2.11)	0.601
Urea, mg/dL	80.5 (± 29.9)	64.4 (± 51.9)	0.281
Creatinine, mg/dL	2.2 (± 2.14)	1.21 (± 0.815)	0.129
Sodium, mEq/L	138 (± 1.85)	137 (± 1.99)	1
AST, units/L	35.6 (± 28.1)	18.7 (± 5.38)	0.145
ALT, units/L	30.3 (± 26.5)	17 (± 8.49)	0.442
Bilirubin, mg, dL	1.0 (± 0.92)	1.21 (± 0.85)	0.52
Alkaline phosphatase, units/L	106 (± 43.9)	76 (± 8.28)	0.127
γ-GT, units	97.6 (± 68.7)	98.7 (± 62.8)	0.897
Drugs	–	–	–
ACEI	2 (25%)	1 (14.29%)	0.4
ARB	2 (25%)	3 (42.86%)	0.175
β-blocker	8 (100%)	4 (57.16%)	0.155
Spironolactone	6 (75%)	7 (100%)	0.509
Loop diuretic	6 (75%)	6 (85.71%)	1
Thiazide diuretic	1 (12.5%)	1 (14.29%)	1
Hydralazine/nitrate	4 (50%)	1 (14.29%)	0.36
Digoxin	2 (25%)	0 (0%)	0.509
Amiodarone	5 (62.5%)	1 (14.29%)	0.17
Rassi score ^c	14.8 (± 2.2)	–	–
Cardiac devices ^d	5 (62.5%)	2 (28.58%)	0.23

Table 1. Baseline characteristics of CCC and IDC patients. Data are expressed as mean (± standard deviation) or as number (%). ACEI angiotensin-converting-enzyme inhibitors, ALT alanine aminotransferase, ARB angiotensin II receptor blockers, AST aspartate transaminase, BMI body mass index, CCC chronic chagasic cardiomyopathy, GT glutamyl transferase, IDC idiopathic dilated cardiomyopathy, LVDD left ventricular diastolic diameter, LVEF left ventricular ejection fraction, NYHA New York Heart Association, O₂ oxygen. ^aFunctional classification according to symptom severity. ^bStratification by degree of congestion and adequacy of perfusion. ^cRiski score for predicting death in patients with CCC. ^dImplantable cardioverter defibrillators, pacemakers and cardiac resynchronization therapy (biventricular pacing).

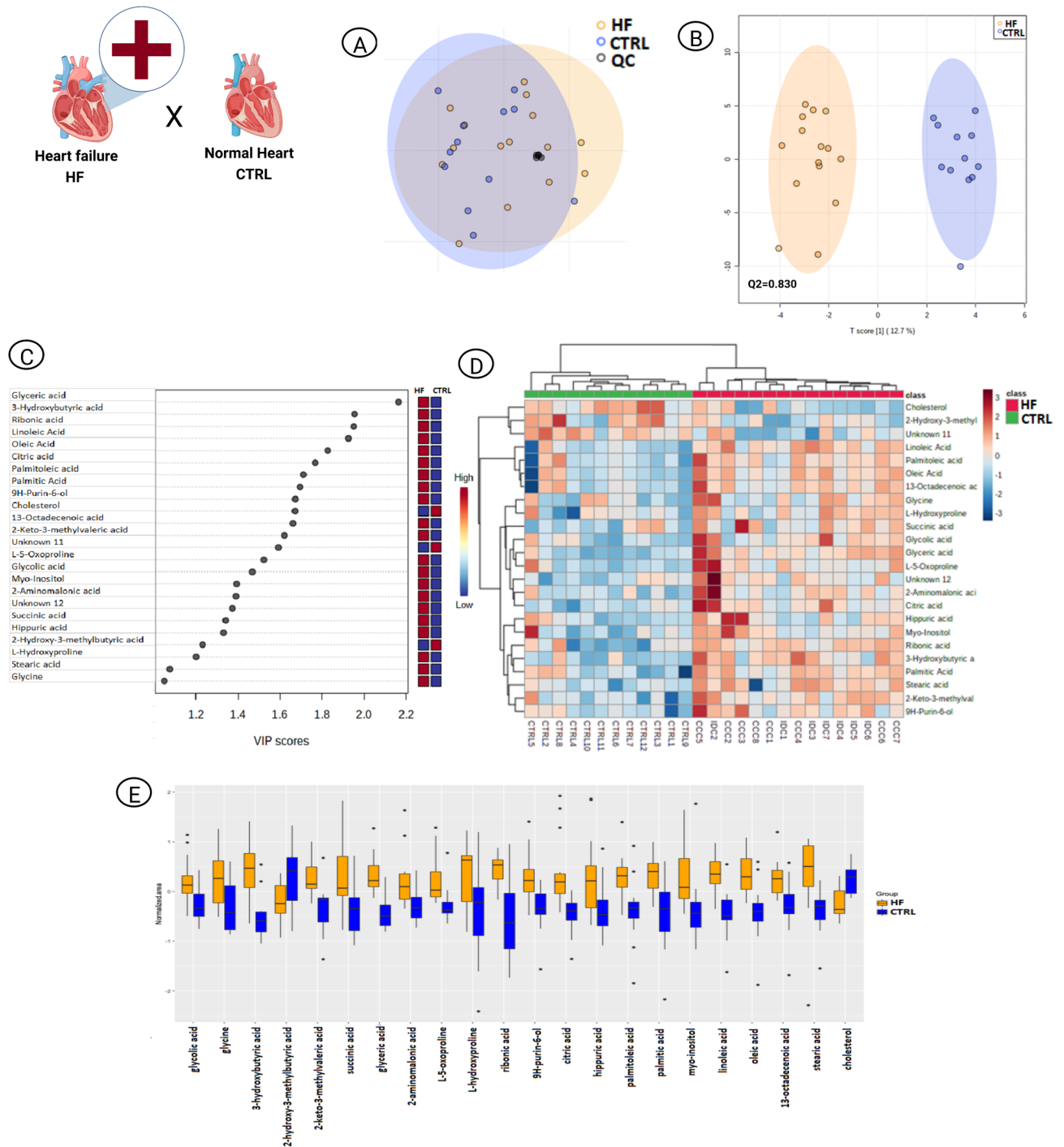


Figure 1. Multivariate analysis of advanced HF^(CCC+IDC) and CTRL patients. **(A)** PCA scores plot to evaluate analytical (QC) reproducibility. **(B)** OPLS-DA scores plot (95% confidence; $p < 0.05$). Each point corresponds to a patient's sample. **(C)** OPLS-DA VIP scores. The colored boxes on the right indicate the relative intensities of the metabolites in each phenotypic group. **(D)** Heatmap hierarchical clustering of the OPLS-DA discriminant metabolites ($VIP \geq 1.0$). Arrays express samples or metabolites relationship. **(E)** Whiskers box plot of OPLS-DA discriminant metabolites ($VIP \geq 1.0$). The diagram shows the compounds distribution in quartiles for each condition and each point outside the range corresponds to an outlier sample. CTRL control, HF heart failure, OPLS-DA orthogonal partial least square discriminant analysis, PCA principal component analysis, QC quality control, VIP variable importance in projection.

expression profiles of CCC and IDC myocardial tissues, reported that several immune response, lipid metabolism and mitochondrial oxidative phosphorylation genes were specifically up-regulated in CCC, with a prominence

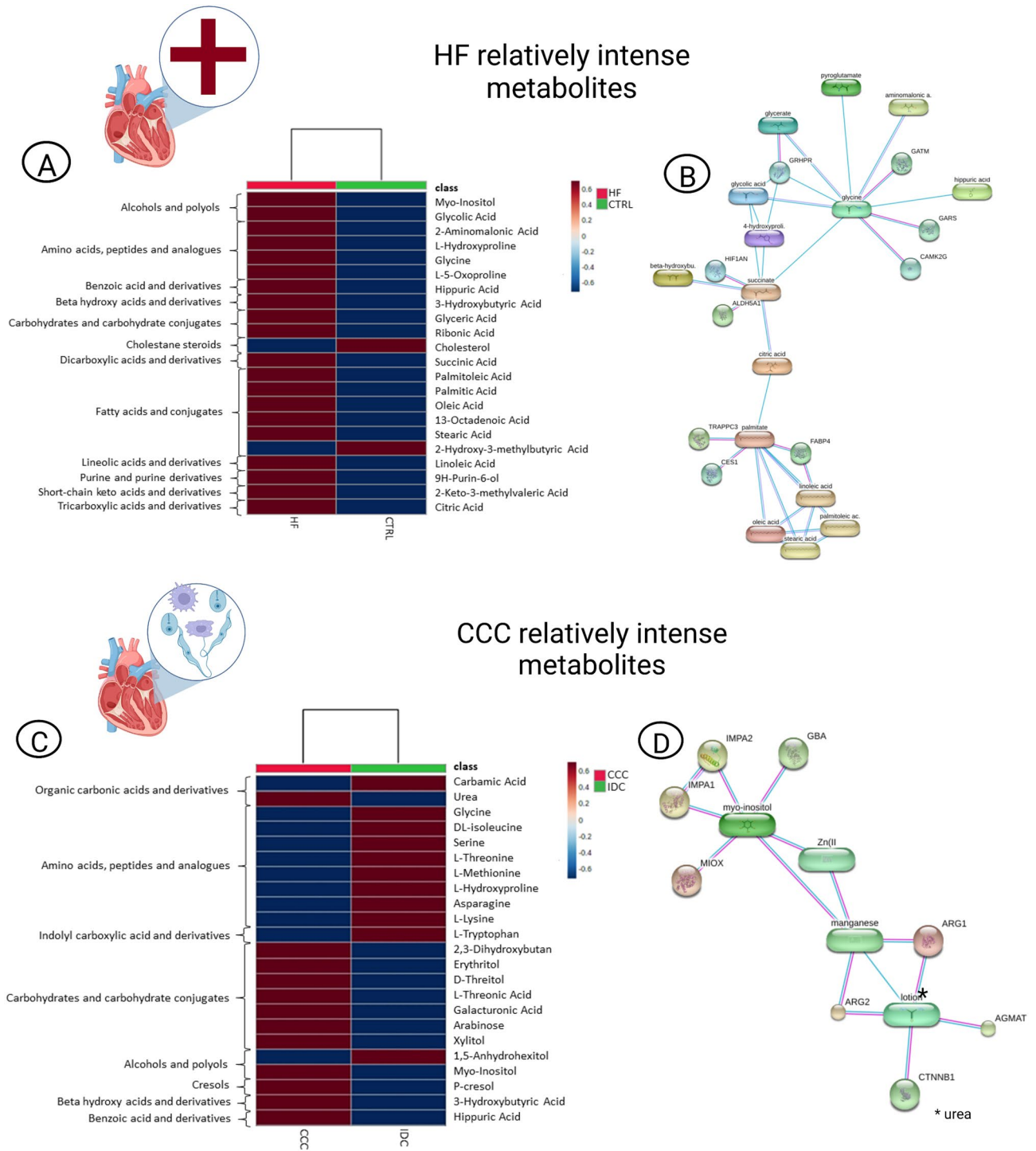


Figure 2. Metabolite network associated with advanced HF^(CCC+IDC) and CCC. **(A)** Heatmap class clustering of HF-discriminating metabolites in OPLS-DA (VIP score ≥ 1.0 , HF vs. CTRL). **(B)** HF-discriminating metabolites network. **(C)** Heatmap class clustering of CCC-discriminating metabolites in OPLS-DA (VIP score ≥ 1.0 , CCC vs. IDC). **(D)** CCC-discriminating metabolites network. Spherical nodes represent predicted functional partners and line colors indicate the type of interaction evidence, meaning blue for curated databases, pink for experimentally determined and purple for protein homology. CCC chronic chagasic cardiomyopathy, CTRL control, HF heart failure, OPLS-DA orthogonal partial least square discriminant analysis, VIP variable importance in projection.

for interferon-gamma (IFN- γ)-inducible genes. Teixeira et al.²⁸ performing a comparative proteomic study on CCC, IDC and ischemic cardiomyopathy myocardial tissue samples, found that patients with CCC had the lowest

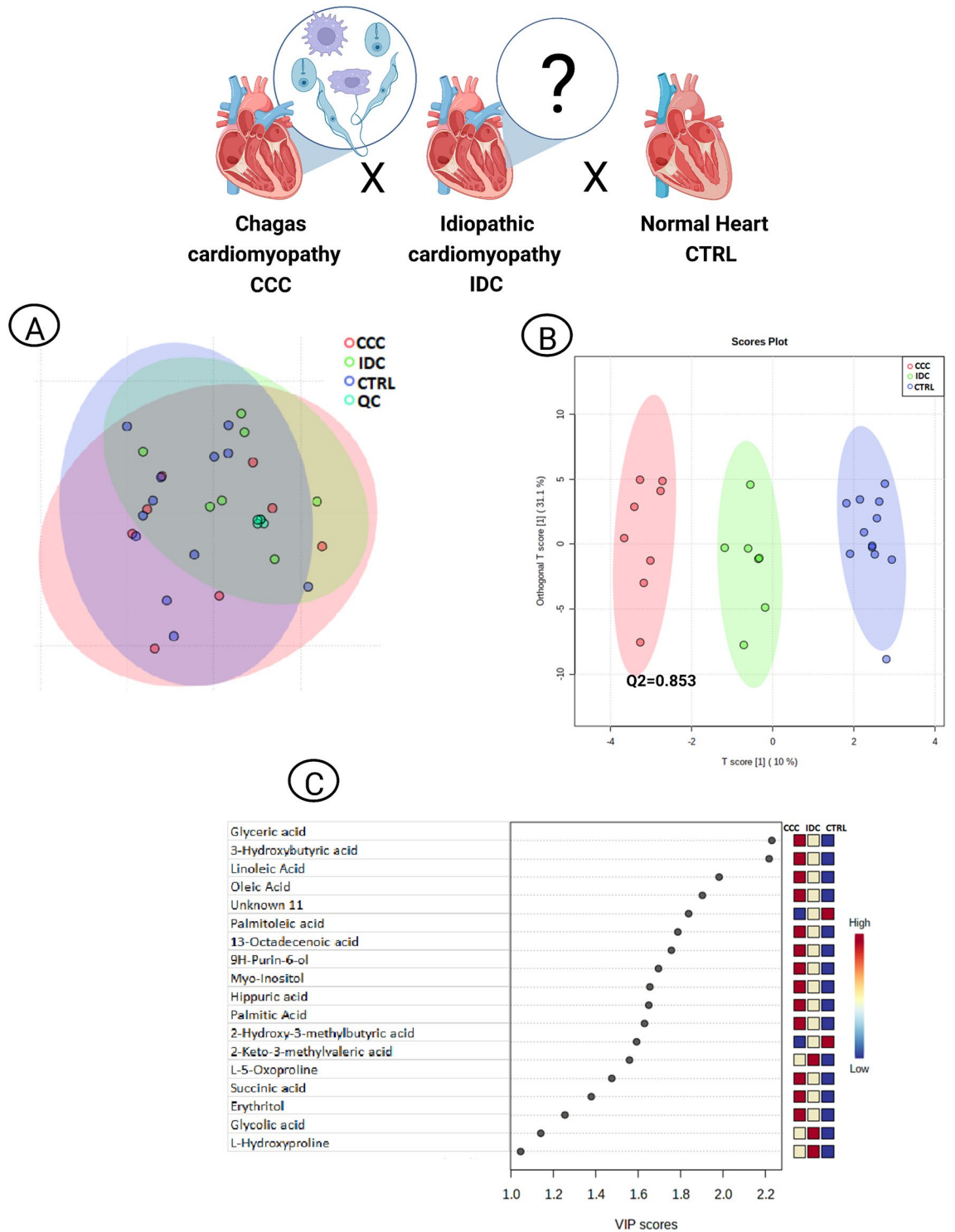


Figure 3. Multivariate analysis of CCC, IDC and CTRL patients. **(A)** PCA scores plot to evaluate analytical (QC) reproducibility. **(B)** OPLS-DA scores plot (95% confidence; $p < 0.05$). Each point corresponds to a patient's sample. **(C)** OPLS-DA VIP scores. The colored boxes on the right indicate the relative intensities of the metabolites in each phenotypic group. CCC chronic chagasic cardiomyopathy, CTRL control, IDC idiopathic dilated cardiomyopathy, OPLS-DA orthogonal partial least square discriminant analysis, PCA principal component analysis, QC quality control, VIP variable importance in projection.

expression of several mitochondrial energy metabolism and FA beta-oxidation proteins, and that high levels of IFN- γ in CCC cardiomyocytes reduce mitochondrial transmembrane potential.

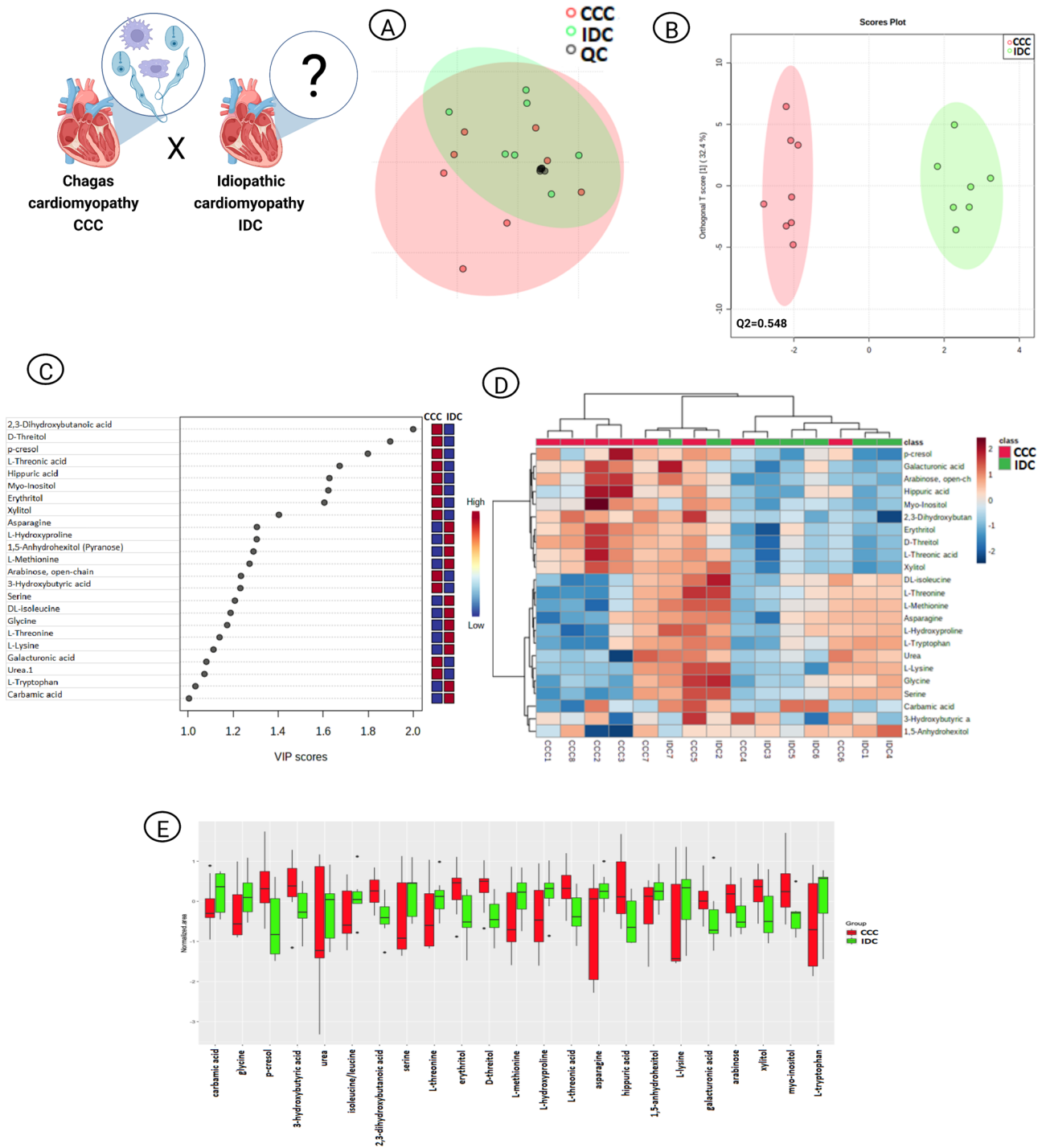


Figure 4. Multivariate analysis of CCC and IDC patients. **(A)** PCA scores plot to evaluate analytical (QC) reproducibility. **(B)** OPLS-DA scores plot (95% confidence; $p < 0.05$). Each point corresponds to a patient's sample. **(C)** OPLS-DA VIP scores. The colored boxes on the right indicate the relative intensities of the metabolites in each phenotypic group. **(D)** Heatmap hierarchical clustering of the OPLS-DA discriminant metabolites (VIP score ≥ 1.0). Arrays express samples or metabolites relationship. **(E)** Whiskers box plot of OPLS-DA discriminant metabolites (VIP score ≥ 1.0). The diagram shows the compounds distribution in quartiles for each condition and each point outside the range corresponds to an outlier sample. CCC chronic chagasic cardiomyopathy, IDC idiopathic dilated cardiomyopathy, OPLS-DA orthogonal partial least square discriminant analysis, PCA principal component analysis, QC quality control, VIP variable importance in projection.

The direct confrontation between CCC and IDC scenarios revealed that, although the predictive ability of OPLS-DA was not as good as the other scenarios – a fact that we attribute to the HF phenotype as a common outcome –, patients with a history of ChD display a distinct metabolic signature (Fig. 4B–E), especially in terms of carbohydrate and AA metabolism (Fig. 2C). Although the selection criteria applied were aimed to minimize the confounding factors, the fact that this was a real-life study did not allow us to reduce the influence of other external factors, such as diet and chronic use of medication, that explain the intensities of xylitol/erythritol and galacturonic acid/arabinose, respectively. Here, such findings are qualitative in nature and were beyond the scope of the present study, but it is advisable that these characteristics be considered in future translational studies.

HF hypercatabolic status is also marked by degradation of skeletal muscle proteins to measure up myocardium dependence on AAs to maintain cardiac ATP levels, leading to cachexia^{29,30}. In HF advanced stages, the reduction of AA levels can also be explained by the development of pathogenic gut flora, reported in more than three quarters of class II to IV patients. Clinically important, this intestinal impairment may alter protein metabolism by reducing intestinal absorptions of vitamin B12, folic acid, and vitamin K³¹. In addition, myocardium remodeling³² and BCAA overconsumption³³ possibly contribute to low AA levels. Wang et al.³⁴ observed that essential AAs plasma levels, except phenylalanine, were lower in patients that had experienced HF-related re-hospitalization or death in comparison to those who did not. Therefore, considering the diverse course of CCC progression compared to other HF etiologies as well, the decrease in the relative intensity of plasma AAs in patients with CCC of the present study may corroborate such indication of disease severity.

More specifically looking at AAs that have been observed as discriminant between the pathological conditions in our work, CCC patients exhibited lower levels of threonine, previously reported by Hennig et al.³⁵. Among other metabolic changes, their fingerprinting approach revealed that threonine levels of rat myoblast were completely depleted in all *T. cruzi* infected conditions, treated with different anti-chagasic drugs or untreated. Similar results were found for *T. brucei procyclic* form, in which threonine is the AA most rapidly metabolized by the parasite for lipid biosynthesis³⁶.

Recently, Salem et al.³⁷ found that not only plasma levels of threonine were decreased in HF patients compared to CTRL subjects, but methionine, isoleucine, serine and lysine as well. Methionine in particular, was also classified as an independent and significant predictor of HF in their multivariate regression analysis. In our study, these AAs were also reduced in CCC patients compared to IDC, and according to Aquilani et al.³³ both AAs number and reduced arterial rates are related to HF severity, thus corroborating the distinct outcome in ChD-related HF. Likewise, the authors also highlighted that methionine levels progressively decrease as the disease worsens.

Tryptophan (Trp) levels also differed between the two HF etiologies in our experiments, with lower intensity in CCC patients. Trp is an essential AA particularly important for proliferation of intracellular pathogens, such as *T. cruzi* amastigotes during the chronic phase of ChD. Host cell dependence on Trp leads to a susceptibility to Trp deprivation by indoleamine 2,3 dioxygenase (IDO)-mediated degradation³⁸. However, Trp starvation together with the accumulation of its active catabolite products (kynurenines) can inhibit proliferation, or promote T cell anergy and death, and modulate helper T cell response^{39–42}. Reinforcing this double-edged sword effect. Marañón et al.⁴³ revealed that IDO activity is higher in patients with ChD compared to CTRL subjects and higher in those in symptomatic chronic cardiac or digestive phase than in asymptomatic patients, establishing a correlation between the enzyme activity status and the transition to chronic infection. They also reported that administration of benznidazole, an anti-chagasic medication, decreased IDO activity in symptomatic patients. Thus, this reduced intensity of Trp observed in CCC patients of our study may be a consequence of its catabolism mediated by the ascending enzymatic activity of IDO.

An increase in CCC myo-inositol levels compared to IDC was also evident in our study. Increased expression of IP₃ receptors (IP₃Rs) is a general and key mechanism in the remodeling of Ca²⁺ signaling during heart disease, with an arrhythmogenic effect during ventricular hypertrophy⁴⁴. Considering that inositol phosphates (IPs) are phosphorylated derivatives of myo-inositol, the increase in myo-inositol levels could be part of a compensatory response to provide an alternative pathway for mobilizing intracellular Ca²⁺ release in advanced stages of HF, as suggested by Deidda et al.⁴⁵. In compliance, Mijares et al.⁶ showed that IP₃R activators induced a greater elevation of diastolic Ca²⁺ in Chagas' cardiomyocytes compared to those of non-chagasic individuals. Furthermore, Chagas' cardiomyocytes had a reduced sarcoplasmic reticulum Ca²⁺ loading, higher level of intracellular IP₃, and compromised contractile properties as well, correlating to (New York Heart Association) NYHA classifications.

CCC patients also had increased levels of urea and hippuric acid compared to the IDC group (Fig. 2C and 4C). Together with our complementary investigations on CCC relatively intense metabolites interaction network (Fig. 2D), these results suggest the hypothesis that the urea cycle of detoxification may be unusually overloaded in ChD-related HF, thereby contributing to the severity of the condition as renal dysfunction is considered an independent outcome predictor in HF^{46–48}. Although such research is beyond the planned scope of the present study, there is indeed an interrelationship between heart and kidney injuries clinically described as cardiorenal syndrome (CRS), which leads to an accumulation of uremic toxins in the body⁴⁹. Applied to the cardiologist's practice, CRS is common in HF patients, associated with worse prognosis and secondary to multiple pathophysiological mechanisms, such as hemodynamic changes leading to venous renal congestion⁵⁰. Moreover, unbalanced protein metabolism in association to kidneys impairment may also culminate in uremia, condition in which levels of urea, myo-inositol and hippuric acid are knowingly increased^{51,52}.

Still on uremic toxins, our data show that p-cresol levels, which is an end product of protein metabolism, were increased in CCC patients compared to the IDC group. In line with our findings, a growing number of publications have confirmed that renal patients revealed an emerging role for this specific metabolite in cardiovascular disease and mortality^{53,54}. In ChD particularly, Gironès et al.⁵⁵ revealed a marked increase of p-cresol in both heart tissue and plasma of *T. cruzi* infected mice, suggesting that alterations in p-cresol metabolism may be associated with increased cardiac stress in acute myocarditis.

In summary, our data reveal novel metabolomic insights into HF molecular events that drive the distinct clinical course of CCC patients from those with non-ischemic DCM. Although impairment of mitochondrial oxidative capacity may be a central mechanistic event in predisposing to HF (Fig. 5A), the associated metabolic imbalance differs between CCC and IDC populations especially in terms of AA metabolism. Tryptophan, methionine, isoleucine, serine and lysine had lower abundance in CCC samples compared to IDC. On the other hand, some uremic toxins, such as urea, hippuric acid and p-cresol were more intense in CCC, possibly indicating an overload of the urea detoxification cycle. Myo-inositol, also known to be implicated in the intracellular remodeling of Ca^{2+} signaling and arrhythmias occurrence, was also more intense in ChD-related advanced HF (Fig. 5B).

From a translational perspective, understanding the functionality of these effector-metabolites in CCC may deepen our knowledge on the metabolic changes that significantly influence the cardiomyopathy development, progression and outcome. We recognize that the number of patients in each biological scenario is not ideal, which may have impacted the analysis of clinical data and pairing of participating patients. Nonetheless, the variables analyzed in this pilot work (metabolites) are excellent discriminant in two of the proposed scenarios ($Q2 > 0.8$). We also acknowledge that a validation of these findings with a larger cohort is needed, in order to translate these important findings into clinics. Future studies should consider including patients with ChD and CCC at various stages to add prognostic value to this matter.

Patients and methods

Study population and experimental design

The present investigation was carried out as a prospective pilot study designed in a real-life context to test the adequacy of plasma metabolomic profiling for differentiating advanced non-ischemic and ChD-related HF. Patients enrolled in the specialized HF program at the Institute of Cardiology and Transplantation of the Federal District (ICTDF) in Brasilia, Brazil, between July 2017 and July 2019 were recruited. Those with advanced HF secondary to non-ischemic DCM referred for heart transplantation (HT) were eligible after chagasic and idiopathic etiologies confirmation. All patients were in stage D (refractory to clinical treatment)⁵⁶, had HF with reduced ejection fraction (HFrEF), and belonged to NYHA classes III or IV⁵⁷. Those undergoing retransplantation, aged > 70 years, with significant hypertension, history of acute myocardial infarction, or coronary, valvular, cerebrovascular, peripheral vascular, hepatic and severe pulmonary diseases were excluded. In total, 15 patients with advanced HF were enrolled – 8 patients with CCC and 7 with IDC.

Twelve heart donors representing the CTRL scenario were also included to experimentally reproduce physiological conditions and ultimately discriminate the molecular characteristics particularly associated with

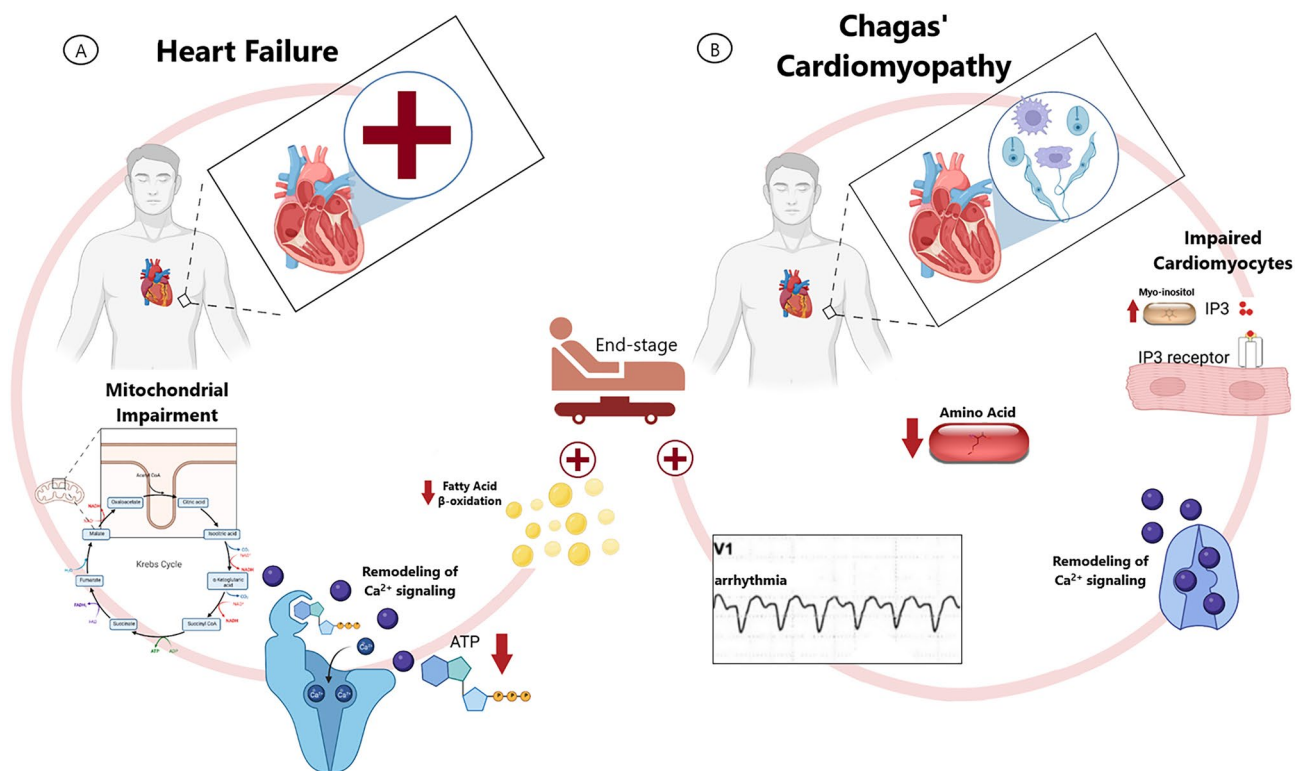


Figure 5. Pathophysiology of advanced HF and CCC from a translational metabolomics basis. **(A)** Link between impaired mitochondrial energy metabolism, FAs and TCA cycle AAs accumulation, LV hypertrophy progression and end-stage HF. **(B)** Link between ChD, impaired cardiomyocytes, higher levels of myo-inositol and intracellular IP_3 , remodeling of Ca^{2+} signaling, arrhythmia and end-stage HF. AA amino acid, Ca^{2+} calcium, CCC chronic chagasic cardiomyopathy, ChD chagas' disease, CTRL control, FA fatty acid, HF heart failure, IP_3 inositol 1,4,5 trisphosphate, LV left ventricle, TCA tricarboxylic acid.

non-ischemic HF, CCC and IDC advanced stages. To preserve the sample collection method, CTRL enrollment criteria included not only the absence of previous or current heart disease, but also referral for evaluation with the same clinical team responsible for HF patients at HT. Heart donors with positive and confirmatory serological tests for ChD, hepatitis B, hepatitis C, syphilis, toxoplasmosis, cytomegalovirus, HIV and/or HTLV I and II were excluded. The study inclusion and exclusion criteria for both HT recipient and donors were based on the recommendations of the International Society for Heart and Lung Transplantation (ISHLT) guideline⁵⁸, 3rd Brazilian heart transplant directive⁵⁹ and Ordinance MS-GM n° 2.600 (October 21, 2009). The selected number of samples included together with the sensitivity of the analytical technique and the complementary assessment of clinical aspects represent, to a lesser extent, a necessary initial step for a larger translational experiment.

Ethics statement

This research was approved by the Ethical Review Committee of the ICTDF, Brasilia, Brazil (13158619.7.0000.0026). Written informed consent was obtained from all participants and all methods were performed in accordance with the relevant guidelines and regulations.

Sample collection and preparation

Peripheral blood samples were collected from the central venous access intraoperatively before heparinization and sternotomy. Following centrifuge-induced fractionation in ethylenediamine tetraacetic acid (EDTA) tubes, 50 μ L aliquots of plasma were diluted in 150 μ L of cold acetonitrile containing 4-nitrobenzoic acid as internal standard. Supernatants aliquots (100 μ L) were lyophilized, reconstituted in 10 μ L of o-methoxyamine hydrochloride in pyridine solution and then added 10 μ L of O-bistrifluoroacetamide (BSTFA) containing 1% chlorotrimethylsilane (TMCS), for derivatization. 4 blank samples, using 50 μ L of Milli-Q® water, and 3 QC samples, consisting of a pool of 100 μ L of each plasma, were also prepared randomly. All sample preparation steps are described in detail in the Supporting Information.

GC–MS/MS analysis

Samples were randomly analyzed by a gas chromatograph (GC 7890A, Agilent Technologies, CA, US) equipped with an automatic liquid sampler (ALS 7693, Agilent Technologies, CA, US) coupled to a quadrupole time-of-flight mass spectrometer (Q-TOF 7200, Agilent Technologies, CA, US). The analysis was performed using a previously developed method⁶⁰ with the analytical conditions described in detail in the Supporting Information.

Data processing and analysis

After spectral deconvolution in Unknowns Analysis software (Agilent Technologies, CA, US), all GC–MS raw data were checked using MassHunter Qualitative software (version 10.0) to determine the data quality, the system mass accuracy, and the reproducibility of the QC sample, IS injections and data integration. Putative identification was performed using MassHunter Qualitative software (version B.10.00, Agilent Technologies, CA, US), NIST MS Search (Gaithersburg, MD, US), an in-house library (PCDL) and the Fiehn 2013 and NIST17 databases. Univariate analyzes were conducted using the R statistical language (version 4.1.0) following the packages Nortest, Stats, Onewaytests and Ggplot2^{61,62}. Data normality was assessed by Shapiro–Wilk's test and those with parametric distribution were tested for heteroscedasticity (F test) and by an appropriate analysis of variance (ANOVA). Non-parametric data were compared by Kruskal–Wallis test. Tukey's and Dunn's post hoc tests, for parametric and non-parametric data, respectively, examined the differences between all paired combinations of groups. Multivariate statistics were conducted in parallel in MetaboAnalyst 4.0⁶³ using the same normalized data matrix. Metabolites of greater contribution to OPLS–DA scenarios were also evaluated by STITCH⁶⁴ targeting the highest confidence score (0.900) in neighborhood. All the data processing steps are described in detail in the Supporting Information.

Data availability

The dataset generated for this study can be found in the MassIVE repository under the link <https://massive.ucsd.edu/ProteomeSAFe/dataset.jsp?task=b30335722ed249afa57e600941f560aa>.

Received: 26 July 2023; Accepted: 6 February 2024

Published online: 29 April 2024

References

- Ikegami, R., Shimizu, I., Yoshida, Y. & Minamino, T. Metabolomic analysis in heart failure. *Circ. J.* **82**, 10–16 (2018).
- Pinto, Y. M. *et al.* Proposal for a revised definition of dilated cardiomyopathy, hypokinetic non-dilated cardiomyopathy, and its implications for clinical practice: A position statement of the ESC working group on myocardial and pericardial diseases. *Eur. Heart J.* **37**, 1850–1858 (2016).
- Dadson, K., Hauck, L. & Billia, F. Molecular mechanisms in cardiomyopathy. *Clin. Sci.* **131**, 1375–1392 (2017).
- World Health Organization. Chagas disease (American trypanosomiasis). *World Health Organization* https://www.who.int/health-topics/chagas-disease#tab=tab_1 (2022).
- Marin-Neto, J. A., Cunha-Neto, E., Maciel, B. C. & Simões, M. V. Pathogenesis of chronic chagas heart disease. *Circulation* **115**, 1109–1123 (2007).
- Mijares, A., Espinosa, R., Adams, J. & Lopez, J. R. Increases in [IP3]i aggravates diastolic [Ca²⁺] and contractile dysfunction in chagas' human cardiomyocytes. *PLoS Negl. Trop. Dis.* **14**, e0008162 (2020).
- Casares-Marfil, D. *et al.* A genome-wide association study identifies novel susceptibility loci in chronic Chagas cardiomyopathy. *Clin. Infect. Dis.* **11**, 617–664 (2021).
- Ferreira, L. R. P. *et al.* Blood gene signatures of Chagas cardiomyopathy with or without ventricular dysfunction. *J. Infect. Dis.* **215**, 387–395 (2017).

9. Cunha-Neto, E., Teixeira, P. C., Fonseca, S. G., Bilate, A. M. & Kalil, J. Myocardial gene and protein expression profiles after auto-immune injury in Chagas' disease cardiomyopathy. *Autoimmun. Rev.* **10**, 163–165 (2011).
10. Cardoso, J. *et al.* Chagas' cardiomyopathy: Prognosis in clinical and hemodynamic profile. *C. Arq. Bras. Cardiol.* **95**, 518–523 (2010).
11. Lopaschuk, G. D., Karwi, Q. G., Tian, R., Wende, A. R. & Abel, E. D. Cardiac energy metabolism in heart failure. *Circ. Res.* **128**, 1487–1513 (2021).
12. Wisneski, J. A., Stanley, W. C., Neese, R. A. & Gertz, E. W. Effects of acute hyperglycemia on myocardial glycolytic activity in humans. *J. Clin. Investig.* **85**, 1648–1656 (1990).
13. Karwi, Q. G., Uddin, G. M., Ho, K. L. & Lopaschuk, G. D. Loss of metabolic flexibility in the failing heart. *Front. Cardiovasc. Med.* **5**, 68 (2018).
14. Yamamoto, T. & Sano, M. Deranged myocardial fatty acid metabolism in heart failure. *Int. J. Mol. Sci.* **23**, 996 (2022).
15. Allard, M. F., Schonekess, B. O., Henning, S. L., English, D. R. & Lopaschuk, G. D. Contribution of oxidative metabolism and glycolysis to ATP production in hypertrophied hearts. *Am. J. Physiol. Hear. Circ. Physiol.* **267**, H742–H750 (1994).
16. Randle, P. J., Garland, P. B., Hales, C. N. & Newsholme, E. A. The glucose fatty-acid cycle: Its role in insulin sensitivity and the metabolic disturbances of diabetes mellitus. *Lancet* **281**, 785–789 (1963).
17. Starling, R. C., Hammer, D. F. & Altschuld, R. A. Human myocardial ATP content and in vivo contractile function. *Mol. Cell. Biochem.* **180**, 171–177 (1998).
18. Zhou, B. & Tian, R. Mitochondrial dysfunction in pathophysiology of heart failure. *J. Clin. Investig.* **128**, 3716–3726 (2018).
19. Bornstein, A. B., Rao, S. S. & Marwaha, K. Left ventricular hypertrophy. In *StatPearls [Internet]. Treasure Island* (eds Bornstein, A. B. *et al.*) (StatPearls Publishing, 2021).
20. Øie, E. *et al.* Fatty acid composition in chronic heart failure: Low circulating levels of eicosatetraenoic acid and high levels of vacenic acid are associated with disease severity and mortality. *J. Intern. Med.* **270**, 263–272 (2011).
21. Yu, Y. *et al.* Serum free fatty acids independently predict adverse outcomes in acute heart failure patients. *Front. Cardiovasc. Med.* **8**, 761537 (2021).
22. Hu, Q. *et al.* Increased Drp1 acetylation by lipid overload induces cardiomyocyte death and heart dysfunction. *Circ. Res.* **126**, 456–470 (2020).
23. Sharma, S. *et al.* Intramyocardial lipid accumulation in the failing human heart resembles the lipotoxic rat heart. *FASEB J.* **18**, 1692–1700 (2004).
24. Barbosa, A. P., Cardinalli Neto, A., Otaviano, A. P., Rocha, B. F. & Bestetti, R. B. Comparison of outcome between chagas cardiomyopathy and idiopathic dilated cardiomyopathy. *Arq. Bras. Cardiol.* **97**, 517–525 (2011).
25. Bestetti, R. B. & Muccillo, G. Clinical course of chagas' heart disease: A comparison with dilated cardiomyopathy. *Int. J. Cardiol.* **60**, 187–193 (1997).
26. Braga, J. C. V. *et al.* Clinical and therapeutics aspects of heart failure due to Chagas disease. *Arq. Bras. Cardiol.* **86**, 297–302 (2006).
27. Cunha-Neto, E. *et al.* Cardiac gene expression profiling provides evidence for cytokinopathy as a molecular mechanism in chagas' disease cardiomyopathy. *Am. J. Pathol.* **167**, 305–313 (2005).
28. Teixeira, P. C. *et al.* Impairment of multiple mitochondrial energy metabolism pathways in the heart of chagas disease cardiomyopathy patients. *Front. Immunol.* **12**, 755782 (2021).
29. Carubelli, V. *et al.* Amino acids and derivatives, a new treatment of chronic heart failure?. *Heart Fail. Rev.* **20**, 39–51 (2015).
30. Krysztofciak, H. *et al.* Cardiac cachexia: A well-known but challenging complication of heart failure. *Clin. Interv. Aging* **15**, 2041–2051 (2020).
31. Pasini, E. *et al.* Pathogenic gut flora in patients with chronic heart failure. *JACC Hear. Fail.* **4**, 220–227 (2016).
32. Lai, L. *et al.* Energy metabolic reprogramming in the hypertrophied and early stage failing heart. *Circ. Hear. Fail.* **7**, 1022–1031 (2014).
33. Aquilani, R. *et al.* Plasma amino acid abnormalities in chronic heart failure: mechanisms, potential risks and targets in human myocardium metabolism. *Nutrients* **9**, 1251 (2017).
34. Wang, C.-H., Cheng, M.-L. & Liu, M.-H. Simplified plasma essential amino acid-based profiling provides metabolic information and prognostic value additive to traditional risk factors in heart failure. *Amino Acids* **50**, 1739–1748 (2018).
35. Hennig, K. *et al.* Metabolomics, lipidomics and proteomics profiling of myoblasts infected with *Trypanosoma cruzi* after treatment with different drugs against chagas disease. *Metabolomics* **15**, 117 (2019).
36. Millerieux, Y. *et al.* The threonine degradation pathway of the *Trypanosoma brucei* procyclic form: The main carbon source for lipid biosynthesis is under metabolic control. *Mol. Microbiol.* **90**, 114–129 (2013).
37. Saleem, T. H., Algowhary, M., Kamel, F. E. M. & El-Mahdy, R. I. Plasma amino acid metabolomic pattern in heart failure patients with either preserved or reduced ejection fraction: The relation to established risk variables and prognosis. *Biomed. Chromatogr.* **35**, e5012 (2021).
38. Cerbán, F. M. *et al.* Signaling pathways that regulate *Trypanosoma cruzi* infection and immune response. *Biochim. Biophys. Acta Mol. Basis Dis.* **1866**, 165707 (2020).
39. Fallarino, F. *et al.* T cell apoptosis by tryptophan catabolism. *Cell Death Differ.* **9**, 1069–1077 (2002).
40. Munn, D. H. *et al.* GCN2 kinase in T cells mediates proliferative arrest and energy induction in response to indoleamine 2,3-dioxygenase. *Immunity* **22**, 633–642 (2005).
41. Frumento, G. *et al.* Tryptophan-derived catabolites are responsible for inhibition of T and natural killer cell proliferation induced by indoleamine 2,3-dioxygenase. *J. Exp. Med.* **196**, 459–468 (2002).
42. Terness, P. *et al.* Inhibition of allogeneic T cell proliferation by indoleamine 2,3-dioxygenase-expressing dendritic cells. *J. Exp. Med.* **196**, 447–457 (2002).
43. Marañón, C. *et al.* Benznidazole treatment reduces the induction of indoleamine 2,3-dioxygenase (IDO) enzymatic activity in chagas disease symptomatic patients. *Parasite Immunol.* **35**, 180–187 (2013).
44. Harzheim, D. *et al.* Increased InsP3Rs in the junctional sarcoplasmic reticulum augment Ca²⁺ transients and arrhythmias associated with cardiac hypertrophy. *Proc. Natl. Acad. Sci.* **106**, 11406–11411 (2009).
45. Deidda, M. *et al.* Metabolomic approach to profile functional and metabolic changes in heart failure. *J. Transl. Med.* **13**, 297 (2015).
46. Costanzo, M. R. The cardiorenal syndrome in heart failure. *Heart Fail. Clin.* **16**, 81–97 (2020).
47. Tabucanon, T. & Tang, W. H. W. Right heart failure and cardiorenal syndrome. *Cardiol. Clin.* **38**, 185–202 (2020).
48. Owan, T. E. *et al.* Secular trends in renal dysfunction and outcomes in hospitalized heart failure patients. *J. Card. Fail.* **12**, 257–262 (2006).
49. Falconi, C. A. *et al.* Uremic toxins: An alarming danger concerning the cardiovascular system. *Front. Physiol.* **12**, 686249 (2021).
50. Ronco, C., Cicoira, M. & McCullough, P. A. Cardiorenal syndrome type 1. *J. Am. Coll. Cardiol.* **60**, 1031–1042 (2012).
51. Lau, W. L. & Vaziri, N. D. Urea, a true uremic toxin: The empire strikes back. *Clin. Sci.* **131**, 3–12 (2017).
52. Clements, R. S., DeJesus, P. V. & Winegrad, A. I. Raised plasma-myoinositol levels in uraemia and experimental neuropathy. *Lancet* **1**, 1137–1141 (1973).
53. Barreto, F. C. *et al.* Serum indoxyl sulfate is associated with vascular disease and mortality in chronic kidney disease patients. *Clin. J. Am. Soc. Nephrol.* **4**, 1551–1558 (2009).
54. Lin, C.-J. *et al.* Serum protein-bound uraemic toxins and clinical outcomes in haemodialysis patients. *Nephrol. Dial. Transplant.* **25**, 3693–3700 (2010).

55. Gironès, N. *et al.* Global metabolomic profiling of acute myocarditis caused by *Trypanosoma cruzi* infection. *PLoS Negl. Trop. Dis.* **8**, e3337 (2014).
56. Hunt, S. A. *et al.* 2009 Focused update incorporated into the ACC/AHA 2005 guidelines for the diagnosis and management of heart failure in adults. *J. Am. Coll. Cardiol.* **53**, e1–e90 (2009).
57. New York Heart Association, Criteria Committee. *Nomenclature and criteria for diagnosis of diseases of the heart and great vessels. Nomenclature and Criteria for Diagnosis of Diseases of the Heart and Great Vessels* (Little (Brown & Co, 1994).
58. Mehra, M. R. *et al.* The 2016 International Society for heart lung transplantation listing criteria for heart transplantation: A 10-year update. *J. Hear. Lung Transplant.* **35**, 1–23 (2016).
59. Bacal, F. *et al.* III Diretriz brasileira de transplante cardíaco. *Arq. Bras. Cardiol.* **111**, 230–289 (2018).
60. Raczkowska, B. A. *et al.* Gas chromatography–mass spectroscopy-based metabolomics analysis reveals potential biochemical markers for diagnosis of gestational diabetes mellitus. *Front. Pharmacol.* **12**, 770240 (2021).
61. Dag, O., Dolgun, A. & Konar, N. M. onewaytests: An R package for one-way tests in independent groups designs. *R J.* **10**, 175–199 (2018).
62. Wickham, H. ggplot2. *WIREs Comput. Stat.* **3**, 180–185 (2011).
63. Chong, J. *et al.* MetaboAnalyst 4.0: Towards more transparent and integrative metabolomics analysis. *Nucleic Acids Res.* **46**, W486–W494 (2018).
64. Kuhn, M. *et al.* STITCH 2: An interaction network database for small molecules and proteins. *Nucleic Acids Res.* **38**, D552–D556 (2010).

Acknowledgements

Authors acknowledge University of San Pablo CEU and CEMBIO staff, especially Vanesa A Herranz, the Cardiac Surgery Service team at ICTDF and financial support from Airbus (scientific agreement EADS CASA 002/DCTA-COPAC/2014).

Author contributions

Study conception: M.U.B.P., F.A.A., A.M.A.M.; infrastructure support: C.B., F.J.R., F.A.A.; funding support: C.B., F.J.R.; sample collection: R.M.O., D.V.N.P., F.A.A.; patients' data collection: R.M.O., M.U.B.P.; experiment development: C.R.C.P., A.M.A.M., C.B., F.J.R.; data interpretation: R.M.O., M.U.B.P., C.R.C.P., D.V.N.P., C.A.O.R., F.A.A., A.M.A.M.; manuscript preparation: R.M.O., M.U.B.P.; figures conception: A.M.A.M.; final revision: R.M.O., M.U.B.P., C.R.C.P., C.A.O.R., C.B., F.J.R., F.A.A., A.M.A.M.; supervision: F.A.A., A.M.A.M.

Competing interests

The authors declare no competing interests.

Additional information

Supplementary Information The online version contains supplementary material available at <https://doi.org/10.1038/s41598-024-53875-7>.

Correspondence and requests for materials should be addressed to A.M.A.M.

Reprints and permissions information is available at www.nature.com/reprints.

Publisher's note Springer Nature remains neutral with regard to jurisdictional claims in published maps and institutional affiliations.



Open Access This article is licensed under a Creative Commons Attribution 4.0 International License, which permits use, sharing, adaptation, distribution and reproduction in any medium or format, as long as you give appropriate credit to the original author(s) and the source, provide a link to the Creative Commons licence, and indicate if changes were made. The images or other third party material in this article are included in the article's Creative Commons licence, unless indicated otherwise in a credit line to the material. If material is not included in the article's Creative Commons licence and your intended use is not permitted by statutory regulation or exceeds the permitted use, you will need to obtain permission directly from the copyright holder. To view a copy of this licence, visit <http://creativecommons.org/licenses/by/4.0/>.

© The Author(s) 2024